COMMUNICATION

# A Hg(I) corrugated sheet assembled by adjuvant dioxole groups and Hg···π interactions

Received 11th March 20xx,
Accepted 00th January 20xx

DOI: 10.1039/x0xx00000x

Francisco Sánchez-Férez,[a] Xavier Solans-Monfort,[a] Teresa Calvet,[b] Mercè Font-Bardia,[c] and Josefina Pons*[a]

**The formation of a new double-stranded staircase Hg(I) supramolecular assembly is reported. It is arranged into 2D corrugated sheets supported by Hg(I)-$O_{dioxole}$ and Hg···π interactions, and resulting from the comproportionation reaction between Hg(II) and Hg(0) species in DMF as solvent.**

Hg as a metal has the particularity of being capable to form a sort of divalent, trivalent and tetravalent polycations arranged either into linear $[Hg_2]^{2+}$ dimeric, $[Hg_3]^{2+}$ trimeric, $[Hg_4]^{2+}$ tetrameric and $[Hg]_n$ chains or into $[Hg_3]^{4+}$ triangles or $[Hg]_n$ layers.[1] All of them present differences in the formation conditions, connectivity, geometry and Hg-Hg distance. In particular, the formation of the $[Hg_2]^{2+}$ dimeric cation is driven by its slightly positive $E^\circ$ value of +0.115 V which facilitates that $Hg^{2+}$ and $Hg^0$ can comproportionate into $Hg_2^{2+}$ as detailed below:[2]

$$Hg^0 + Hg^{2+} \rightarrow Hg_2^{2+} \qquad E^\circ = +0.115\ V$$

This comproportionating ability has been reported to occur in polar solvents, especially in N,N-dimethylformamide (DMF)[3] or by strong Lewis bases *inter alia O*- and *N*-donor ligands.[4,5] Although intrinsic reduction of Hg(II) at high temperature is uncommon, there are previously reported examples in the mentioned conditions.[4] DMF under high temperature can act as a reducing agent[6,7] conducting the formation of $Hg^0$ and triggers comproportionation. The complexation of the $[Hg_2]^{2+}$ dimeric cation is usually stabilized by both a lower solubility compared to their Hg(II) analogous and the weakening of the donor character of the ligands that minimize destabilization of the Hg-Hg bond.[8] Correlation between Hg-Hg bond length, ranging from 2.495 to 2.557 Å, and the coordinated atoms, has been attributed to their electronegativity, being shortened as electronegativity increases. In presence of an *O*-donor carboxylate linker, the Hg-Hg distance is enclosed within 2.502-2.557 Å.[1] Hg(I) has a strong tendency to form linear arrays due to its soft nature and it usually adopts low coordination numbers up to four, even though it is capable to accommodate coordination numbers up to seven.[9] This preferred linear arrangement facilitates the formation of metal···π interactions which have proven to be pivotal in defining the arrangement of macromolecules.[10] The electrostatic origin of metal···π interaction made it emerge as one of the strongest noncovalent interactions but this strength is highly dependent on the coordinatively saturation of the metal, the nature of the π donor aromatic ring and cooperativity with other nonbonding interactions as hydrogen bonds or π···π stacking.[10] In the case of $Hg^{2+}$, the almost fully populated d orbitals combined with the large s-d orbital energy splitting hinder the sd hybridization, albeit evidence of d orbitals implication in Hg···π interactions has been reported.[11] For this reason, π to Hg donation generally occurs from the molecular orbitals of the aromatic ring to the unoccupied 6s orbital.[12] This favors delocalized π interactions of Hg with an offset from the centroid ring and placed preferentially over two ($\pi_{off}(2)$) or three carbon atoms ($\pi_c(3)$), and minimize those in which Hg is sitting over the center of the ring ($\pi_{cen}(6)$). These results were braced by a statistical analysis on metal···π interactions which reinforced that transition metals preferred an offset over the center of the ring in delocalized π interactions.[13] Thus far, there are about 28 structures containing the $[Hg_2]^{2+}$ specie being coordinated to *O* atoms.[14] From them, six were constructed from carboxylate linkers *inter alia* two alaninate,[15] one trifluoroacetate,[16] one acetate,[17] one gluconate[18] and one phthalate,[19] all presenting 1D polymeric structures. Above all, only $[Hg_2(o\text{-phthalate})_2]_n$ is arranged through an aromatic carboxylate. Examples of coordinated dioxole groups to metal centers are scarce and only $d^{10}$ metal ions have exhibited such coordination ability. A reported case in the literature with Zn(II)[20] and one found in our

[a] *Departament de Química, Universitat Autònoma de Barcelona, 08193-Bellaterra, Barcelona, Spain*
[b] *Departament de Mineralogia, Petrologia i Geologia Aplicada, Universitat de Barcelona, Martí i Franquès s/n, 08028 Barcelona, Spain.*
[c] *Unitat de Difracció de Raig-X, Centres Científics i Tecnològics de la Universitat de Barcelona (CCiTUB), Universitat de Barcelona, Solé i Sabarís, 1-3, 08028 Barcelona, Spain*

† Electronic Supplementary Information (ESI) available: Experimental details, single crystal data, FTIR-ATR and 1H NMR spectra. CCDC 2155639. For ESI and crystallographic data in .cif or other electronic format see DOI: 10.1039/x0xx00000x

group with Hg(II)[21] have been found hitherto. In our case, Hg(II)···$O_{dioxole}$ and Hg···C interactions promoted the formation of a 2D supramolecular assembly. Therefore, the coordination chemistry and structural arrangement of Hg(I) with aromatic carboxylates has not been extensively explored, even less in presence of dioxole groups. In this work, we provide an example of a Hg(I) aromatic carboxylate complex, which assembles by Hg(I)···$O_{dioxole}$ interactions, further expanded into a 3D supramolecular structure by Hg···π interactions. The formation of the $[Hg_2]^{2+}$ dimeric cation was observed after recrystallization of $[Hg(Pip)_2(4,4'\text{-bipy})]_n$ (**1**) in DMF as solvent at 105°C for 1h.[22] In these conditions the formation of Hg(0) is observed, which combined with the remaining Hg(II) in solution comproportionate to give the $[Hg_2]^{2+}$ specie. The subsequent complexation with Pip ligands results in a less soluble compound that gradually nucleated and formed single crystals of $[Hg_2(Pip)_2]$ (**2**).

Complex **2** has been characterized by elemental analysis, FTIR-ATR and $^1$H NMR spectroscopies (S.I: Fig. S1 and S2), and single crystal X-ray diffraction (see details in the Supporting Information). The deprotonation and subsequent coordination of the Pip linker has been traced by the vanishing of the $\upsilon(C{=}O)_{COOH}$ band and the rising of bands attributable to $\upsilon_{as}(COO)$ at 1580 cm$^{-1}$ and $\upsilon_s(COO)$ at 1431 cm$^{-1}$. The coordination modes of the carboxylate can be inferred by calculating Δ values (Δ = $\upsilon_{as}(COO) - \upsilon_s(COO)$), which were found to be 149 cm$^{-1}$ falling in mid-range between bidentate bridging and bidentate chelate coordination mode.[23] Therefore, this data suggests the presence of both bridging and chelate coordination modes of the Pip units. These results agree with the structural data obtained from the single crystal X-ray diffraction method. The $^1$H NMR spectrum in DMSO-$d_6$ displays the aromatic signals of Pip at 7.53, 7.35 and 6.96 ppm and the -C$H_2$- at 6.08 ppm (free HPip: 7.55, 7.36, 6.99, 6.11 ppm).

Compound **2** crystallizes in the Monoclinic, P21/n space group (S.I: Table S1) and it is composed of linear $[Hg_2(Pip)_2]$ units that hold two monodentate ($\mu_1$-$\eta^1$) Pip ligands (Fig. 1a), with a coordination number of 2 (Hg1-O1, 2.132(2) Å and Hg2-O5, 2.126(2) Å, that are below the sum of their covalent radii of 2.21 Å)[24] displaying a Hg-Hg bond length of 2.51602(18) Å (Fig. 1a), that falls within the reported range between 2.502 and 2.557 Å.[1] Distances below the van der Waals sum of radii (vdWs, from 2.21 to 3.02 Å) have previously been included defining the secondary coordination number, and according to this criteria the coordination number of Hg1 is [2+3] (Hg1 – O2, 2.742(2) Å; Hg1 – O6, 2.782(2) Å; and Hg1 – O5, 3.013(2) Å) and Hg2 is [2+1] (Hg2 – O6, 2.891(2) Å).[25] The $[Hg_2(Pip)_2]$ unit are joined together in tetranuclear $[Hg_4(Pip)_4]$ clusters by Pip ligands through the secondary coordination (2.742(2) Å and 2.891(2) Å) and supported by C-H···O interactions between Pip ligands (Fig. 1b). These $[Hg_4(Pip)_4]$ clusters are further expanded into a 1D double-stranded staircase assembly along *b* axis through Hg1 – O5, 3.013(2) Å (Fig. 2a). This arrangement is supported by delocalized Hg1··· $\pi_{off}(2)$ and Hg2···$\pi_c(3)$ interactions occurring within the supramolecular chains (Fig. 2b), that display highlighted regions over the aromatic rings in the Hirshfeld surface analysis and a 9.6% of Hg···C contact surface area contribution in the 2D fingerprint plot (S.I: Fig. S3). These chains are assembled into 2D corrugated sheets through two Hg(I)-$O_{dioxole}$ interactions (Hg1 – O7, 3.081(2) Å and Hg2 – O4, 3.132 Å) complemented by double C-H···O interactions between the Pip ligands (Fig. 3, Table S2). The importance of metal···π interactions and their effect on the final arrangement have already been demonstrated[10,26] but no results were found regarding $[Hg_2]^{2+}$ cation. A search in the Cambridge Structural Database (CSD)[14] of structures containing the $[Hg_2]^{2+}$ cation and N, O, S and P-donor atoms resulted in 129 hits. Disordered structures were eliminated in order to include only precise crystal structure determinations. This data was sifted through those with aromatic rings and was reduced to a total of 50 entries with potential Hg···π interactions. One requirement is

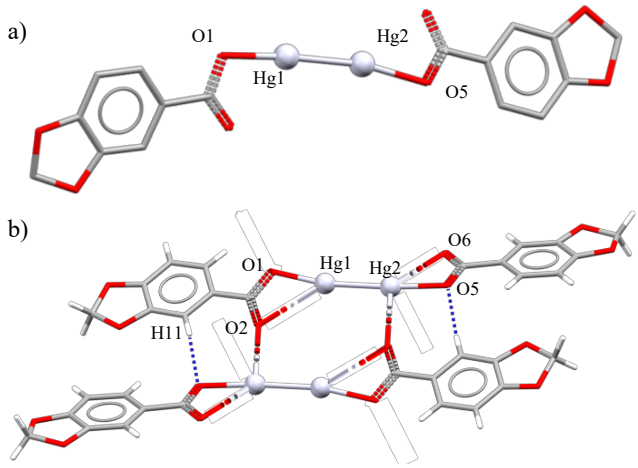


Figure 1. Crystal structure representation of **2**. a) dinuclear $[Hg_2Pip_2]$ units displaying ($\mu_1$-$\eta^1$ coordination modes. b) tetranuclear $[Hg_2Pip_4]$ units supported by Hg··O and C-H···O interactions (represented as dashed lines). Color codes: suva grey (Hg), red(O), grey (C) and white (H).

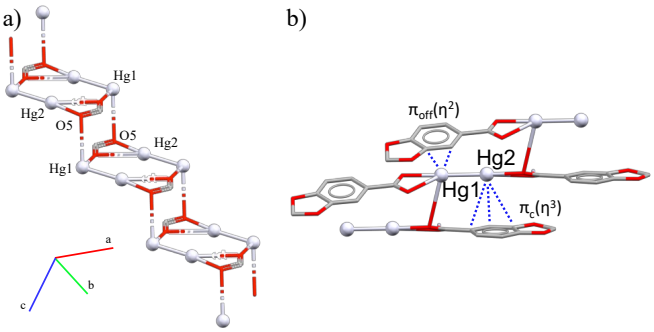


Figure 2. View of the a) 1D double-stranded staircase assembly, and b) Hg1··· $\pi_{off}(\eta^2)$ and Hg2···$\pi_c(\eta^3)$ interactions .

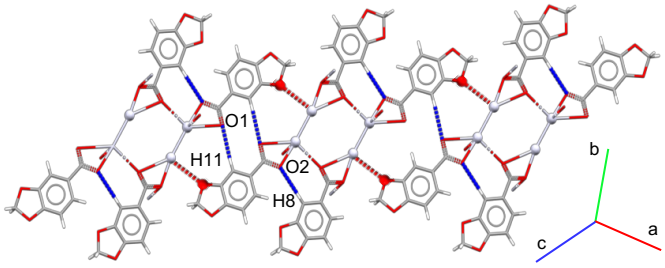


Figure 3. View of the assembly of 2D corrugated sheets supported by Hg···$O_{dioxole}$ and C-H···O interactions.

# COMMUNICATION

Table 1. CSD results of the selected structures exhibiting Hg(I)···π interactions

| Complex | CN[a] | $d_{HgC}$ (Å) | $d_{HgCg}$ (Å) | $d_{HgP}$ (Å) | Offset[b] (Å) | Conformation | Ref. |
|---|---|---|---|---|---|---|---|
| $[Hg_2(Pip)_2]$ (**2**) | 2 | 3.405(3); 3.488(3); 3.358(3); 3.460(3); 3.647(3) | 3.720[c] 3.446[d] | 3.342 3.318 | 1.634 0.9305 | $\pi_{off}(2) + \pi_c(3)$ | This work |
| $[Hg_2(o\text{-phthalate})_2]_n$ (**A**) | 2 | 3.335; 3.419; 3.469; 3.646; 3.687; 3.737 3.341; 3.459 | 3.256[e] 3.801[e] | 3.213 3.217 | 0.5274 2.024 | $\pi_{cen}(6) + \pi_{off}(2)$ | 19 |
| $(Hg_2)Hg_3(O_3P(C_6H_4)PO_3)_2\cdot 2H_2O$ (**B**) | 2 | 3.12(2); 3.41(2); 3.45(2) | 3.424[f] | 3.137 | 1.372 | $\pi_c(3)$ | 27 |
| $Hg_2(N(Ar)(SiMe_3))_2$ (**C**) | 2 | 3.155(3); 3.361(3); 3.458(4) | 3.380[g] | 3.143 | 1.243 | $\pi_c(3)$ | 28 |
| $Hg_2(N(Ar)(SiPr^i_3))_2$ (**D**) | 2 | 3.413(6); 3.458(5) | 3.620[h] | 3.362 | 1.342 | $\pi_{off}(2)$ | |
| $[Hg_2(L^{oPh})]\cdot(ClO_4)_2\cdot(CH_3NO_2)$ (**E**) | 3 | 3.37(3); 3.63(3) | 3.817[i] | 3.301 | 1.917 | $\pi_{off}(2)$ | 29 |
| $[Hg_2(L^{mPh})(DMF)_2]\cdot(ClO_4)_2$ (**F**) | 3 | 3.478(6); 3.672(6); 3.788(8); 3.524(7); 3.575(8); 3.395(8); 3.540(7); | 3.732[j] 3.721[j] 3.836[k] | 3.466 3.476 3.300 | 1.384 1.328 1.956 | $\pi_c(3) + \pi_{off}(2)$ | |
| $[Hg_2(L^{pPh})]\cdot(ClO_4)_2$ (**G**) | 3 | 3.28(1); 3.41(1); 3.62(1); 3.51(1); 3.66(1); 3.30(1); 3.58(1); 3.61(1); | 3.485[l] 3.719[l] 3.628[m] | 3.255 3.497 3.294 | 1.245 1.266 1.521 | $\pi_c(3) + \pi_{off}(2)$ | |
| $[Hg_2((MesNCMe)_2CH)_2]\cdot$hexane (**H**) | 2 | 3.090(4); 3.320(4); 3.510(4); 3.081(4); 3.248(4); 3.452(4); | 3.430[n] 3.322[o] | 3.077 3.060 | 1.516 1.293 | $\pi_c(3)$ | 30 |
| $[Hg_2(TIP)_2](ClO_4)_2$ (**I**) | 3 | 3.338(6); 3.570(7); 3.590(6); 3.428(2); 3.508(6) | 3.519[p] 3.620[q] | 3.331 3.341 | 1.135 1.394 | $\pi_c(3)$ | 31 |

[a]CN = coordination number; [b]offset = $\sqrt{(d_{MC}^2 - d_{MP}^2)}$. $d_{HgC}$ = distance Hg···C atom; $d_{HgCg}$ = distance Hg···centroid, $d_{HgP}$ = distance Hg···plane defined by the aromatic ring; Centroids: [c]C(2)-C(3)-C(4)-C(5)-C(7)-C(8); [d]C(10)-C(11)-C(12)-C(14)-C(15)-C(16); [e]C(2B)-C(3B)-C(4B)-C(5B)-C(6B)-C(7B); [f]C(1A)-C(2A)-C(3A)-C(4A)-C(5A)-C(6A); [g]C(10B)-C(15B)-C(16B)-C(17B)-C(34B)-C(37B); [h]C(10)-C(24)-C(33)-C(40)-C(41)-C(42); [i]C(1)-C(2)-C(3)-C(4)-C(5)-N(1);[j]C(10)-C(11)-C(12)-C(13)-C(14)-C(15); [k]C(1)-C(2)-C(3)-C(4)-C(5)-N(1); [l]C(10)-C(11)-C(12)-C(13)-C(14)-C(15); [m]C(44)-C(45)-C(46)-C(47)-C(48)-N(12); [n]C(15)-C(16)-C(17)-C(18)-C(19)-C(20); [o]C(44)-C(45)-C(46)-C(47)-C(48)-C(49); [p]N(3A)-C(4A)-C(5A)-C(6A)-C(13A); [q]S(1A)-C(14A)-C(15A)-C(16A)-C(17A) . $(O_3P(C_6H_4)PO_3)_2$ = 1,4-phenylenebisphosphonic acid; N(Ar)($SiMe_3$) = N-(2,6-bis(Diphenylmethyl)-4-isopropylphenyl)-1,1,1-trimethylsilanaminato; N(Ar)($SiPr^i_3$) = N-(2,6-bis(Diphenylmethyl)-4-methylphenyl)-1,1,1-tri-isopropylsilanaminato; $L^{oPh}$ = 1,2-bis(3-(2-Pyridyl)pyrazol-1-ylmethyl)benzene-N,N',N'',N'''; $L^{mPh}$ = 1,3-bis(3-(2-Pyridyl)pyrazol-1-ylmethyl)benzene-N,N',N'',N'''; $L^{pPh}$ = 1,4-bis(3-(2-Pyridyl)pyrazol-1-ylmethyl)benzene-N,N',N'',N'''; ($(MesNCMe)_2CH$) = 1,3-bis(2,6-di-isopropylphenyl)-N-(trimethylsilyl)-1,3-dihydro-2H-1,3,2-diazaborol-2-amino; TIP = 2-(2-thienyl)-1H-imidazo[4,5-f][1,10]phenanthroline-$N^7$,$N^8$.

that metal acceptor has a coordinatively unsaturated environment that allows the bulky aromatic ring to get closer.

The vast majority presents crowded structures with coordination numbers of 2 with secondary interactions up to 7 [2+5][9] with solvent molecules either below or over their vdWs, that hinders Hg(I)···π interactions. Besides in some examples the geometric preferences of the ligands hamper the proper orientation of the aromatic rings towards the $[Hg_2]^{2+}$ cation.[5] Of them, only 9 hits presented delocalized π interactions with $[Hg_2]^{2+}$, considering either Hg(I) to benzene plane distance ($d_{HgP}$) below to vdWs of Hg and C atoms (3.45 Å)[11] or Hg(I) to centroid distance below 4.0 Å[13]. For all the structures each Hg···π interaction has been split into the coordination number of the Hg(I) atom, the distances

between Hg and i) the nearest C atoms ($d_{HgC}$); ii) the ring centroid ($d_{HgCg}$); iii) the plane containing the aromatic ring ($d_{HgP}$); the offset, which is defined as $\sqrt{(d_{HgCg}^2-d_{HgP}^2)}$[13] and the conformation[12], resulting in 14 Hg(I)···π interactions. Each interaction with the mentioned parameters has been summarized in Table 1. The general trend is that an offset of the Hg(I) center over sitting in the ring centroid axis is preferred, being $\pi_c(\eta^3)$ slightly favored over $\pi_{off}(2)$. Only $[Hg_2(o\text{-phthalate})_2]_n$ (**A**) presents a small offset of 0.5274 Å and exhibits a $\pi_{cen}(6)$ conformation. Among them, **E**, **G** and **I** present Hg(I)···π···π cooperativity, which is reported to be a prevailing motif by enhancing the strength of the π···π interaction.[10] The $\pi_{off}(2)$ and $\pi_c(3)$ conformations are present in the remaining structures (**B**, **C**, **D**, **F**, **H**) with offset values from 0.9305 to 2.024 Å and between 1.243 and 1.516 Å, respectively. It can be inferred that $\pi_c(3)$ conformation (**B**, **C**, **F**, **G**, **H** and **I**) limits the offset range by anchoring the Hg(I) ion and preventing it to place out of the aromatic ring. The smallest offsets have been found in complexes **2** and **A**, both bearing structures that predispose Hg(I) atoms to sit closer to the centroid of the aromatic ring. Besides, the interaction of the dioxole *O* atoms to Hg1 in **2** reduce Hg···π, resulting in $\pi_{off}(2)$ while the coordinatively unsaturated Hg1 can accommodate the $\pi_c(3)$ interaction.

DFT (B3LYP-D2) calculations have been performed to analyse the interaction between $[Hg_2(Pip)_2]$ dimers. For that, two sets of calculations were carried out: first, a full periodic calculation of the crystal structure to determine the existing interactions through the Bader's Atom In Molecules (QTAIM) theory and, secondly, finite molecular calculations of all potential close $[Hg_2(Pip)_2]$ units to quantify the interaction strength between dimers. Both sets of calculations were done with Crystal17 package, and the basis sets were similar to those used for describing related Hg complexes (See Supplementary Information). Figure 4 shows the four models constructed to determine the interaction strength between dimers, the corresponding interaction energies (with and without Grimme's correction), and the bond critical points (BCP) involving Hg centres. Table S3 reports the main properties for the BCP involving Hg.

The analysis performed with TOPOND located BCPs between the two Hg, the Hg and the nearest O atoms (in-plane COO, out-of-plane -COO and dioxole fragments) as well as a BCP located in between Hg and the closest aromatic ring. The presence of these BCP are indicative of a Hg-Hg, Hg-O and Hg···π

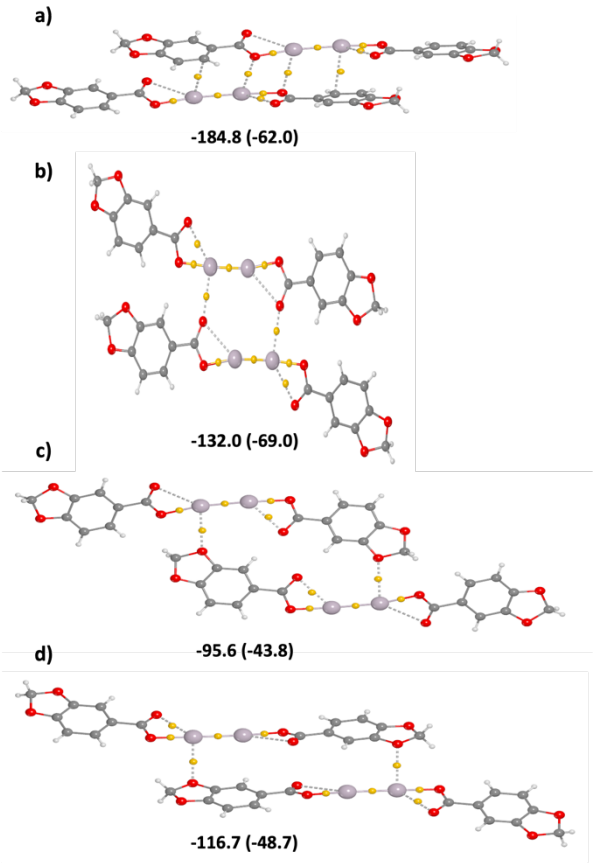


Figure 4. Models constructed to analyse the interaction between dimers and the associated interaction energies (without including dispersion forces in parenthesis). Yellow spots correspond to the BCPs involving Hg cations. Values in kJ $mol^{-1}$

interactions. The electron density and its Laplacian in the BCPs between Hg and the oxygen atoms or Hg and the aromatic ring indicate that the interaction is mainly of electrostatic and/or Van der Waals nature. The computed interaction energies between dimers range from 184.8 and 95.6 kJ $mol^{-1}$. The strongest interaction is found for dimers interacting through both an out-of-plane Hg···$O_{COO}$ and a Hg···π interaction while the weakest interactions take place through the dioxoles. Interestingly, while the Hg···$O_{COO}$ in-plane interaction is marginally stronger than the out-of-plane one (in agreement with the shorter Hg····O distance), the Hg···π interaction, only present in the latter case, is of the same order of magnitude and thus, the staircase stacking is, overall stronger than the in-plane one.

## Conclusions

The use of DMF as solvent and the decomposition of precursor **1** to give Hg(0), has driven the formation of the $[Hg_2]^{2+}$ cation, which after coordination with Pip linker has been stabilized through precipitation by the low solubility of complex **2**. Hg···π interactions cooperate in the formation of the double-stranded staircase chains, which are connected into a 2D sheets by an uncommon Hg(I)-$O_{dioxole}$ interaction. Besides, literature results of Hg(I)···π interactions have been compiled and analyzed, revealing that $\pi_c(3)$ conformation is slightly preferred over $\pi_{off}(2)$ for the $[Hg_2]^{2+}$ cation.

## Author Contributions

Conceptualization, J.P.; data curation, F.S.-F. and M.F.-B.; formal analysis, F.S.-F. and M.F.-B.; funding acquisition, J.P.; investigation, F.S.-F.; methodology, F.S.-F.; project administration, J.P.; resources, T.C. and J.P.; software, F.S.-F.; supervision, J.P.; validation, T.C. and J.P.; visualization, F.S.-F.; writing—original draft, F.S.-F.; writing—review and editing, T.C. and J.P.

## Conflicts of interest

There are no conflicts to declare

## Acknowledgements

J.P. acknowledges financial support from the CB615921 project, the CB616406 project from "Fundació La Caixa" and the 2017SGR1687 project from the Generalitat de Catalunya. F.S.F. acknowledges the PIF pre-doctoral fellowship from the Universitat Autònoma de Barcelona.

## Notes and references

1 L. M. Volkova and S. A. Magarill, *J. Struct. Chem.*, 1999, **40**, 262–269.
2 R. A. Jackson, *The chemistry of mercury*, The Macmillan Press Ltd, London and Basingstoke, 1st editio., 1978.
3 M. Kadarkaraisamy and A. G. Sykes, *Polyhedron*, 2007, **26**, 1323–1330.
4 N. J. Williams, R. D. Hancock, J. H. Riebenspies, M. Fernandes and A. S. De Sousa, *Inorg. Chem.*, 2009, **48**, 11724–11733.
5 D. C. Bebout, J. F. Bush, E. M. Shumann, J. A. Viehweg, M. E. Kastner, D. A. Parrish and S. M. Baldwin, *J. Chem. Crystallogr.*, 2003, **33**, 457–463.
6 J. Muzart, *Tetrahedron*, 2009, **65**, 8313–8323.
7 M. M. Heravi, M. Ghavidel and L. Mohammadkhani, *RSC Adv.*, 2018, **8**, 27832–27862.
8 K. Brodersen, *Comments Inorg. Chem.*, 1981, **1**, 207–225.
9 K. Brodersen and R. Dolling, *Chem. Ber.*, 1978, **111**, 3354–3359.
10 A. S. Mahadevi and G. N. Sastry, *Chem. Rev.*, 2013, **113**, 2100–2138.
11 A. Lannes, A. Manceau, M. Rovezzi, P. Glatzel, Y. Joly and I. Gautier-Luneau, *Dalton Trans.*, 2016, **45**, 14035–14038.
12 H. B. Yi, H. M. Lee and K. S. Kim, *J. Chem. Theory Comput.*, 2009, **5**, 1709–1717.
13 A. Banerjee, A. Saha and B. K. Saha, *Cryst. Growth Des.*, 2019, **19**, 7264–7270.
14 C. R. Groom, I. J. Bruno, M. P. Lightfoot and S. C. Ward, *Acta Crystallogr. Sect. B Struct. Sci. Cryst. Eng. Mater.*, 2016, **72**, 171–179.
15 C. D. L. Saunders, N. Burford, U. Werner-Zwanziger and R. Mcdonald, 2008, **47**, 3693–3699.
16 M. Sikirica and D. Grdenić, *Acta Crystallogr. Sect. B*, 1974, **30**, 144–146.
17 T. J. Prior, *Acta Crystallogr. Sect. E Struct. Reports Online*, 2005, **61**, m1523-1524.
18 I. G. Konkina, S. P. Ivanov and Y. I. Murinov, *Russ. J. Inorg. Chem.*, 2019, **64**, 201–206.
19 B. Lindh, 1967, **21**, 2743–2752.
20 P. V. Dau, L. R. Polanco and S. M. Cohen, *Dalton Trans.*, 2013, **42**, 4013–4018.
21 D. Ejarque, F. Sánchez-Férez, J. A. Ayllón, T. Calvet, M. Font-Bardia and J. Pons, *Cryst. Growth Des.*, 2020, **20**, 383–400.
22 F. Sánchez-Férez, X. Solans-Monfort, T. Calvet, M. Font-Bardia and J. Pons, *Inorg. Chem.*, 2022, **61**, 4965-4979.
23 G. B. Deacon and R. J. Phillips, *Coord. Chem. Rev.*, 1980, **33**, 227–250.
24 J. G. Wright, M. J. Natan, F. M. Macdonnell, D. M. Ralston and T. V. O. Hallorant, in *Progress in Inorganic Chemistry*, ed. S. J. Lippard, John Wiley & Sons, Hoboken, New Jersey, USA, 2007, pp. 323–412.
25 D. Grdenić, *Q. Rev. Chem. Soc.*, 1965, **19**, 303–328.
26 H. Lee, H. S. Lee, J. H. Reibenspies and R. D. Hancock, *Inorg. Chem.*, 2012, **51**, 10904–10915.
27 N. B. Padalwar and K. Vidyasagar, *J. Solid State Chem.*, 2016, **243**, 83–94.
28 J. Hicks, E. J. Underhill, C. E. Kefalidis, L. Maron and C. Jones, *Angew. Chemie - Int. Ed.*, 2015, **54**, 10000–10004.
29 S. P. Argent, H. Adams, T. Riis-Johannessen, J. C. Jeffery, L. P. Harding, W. Clegg, R. W. Harrington and M. D. Ward, *Dalton Trans.*, 2006, 4996–5013.
30 M. Juckel, D. Dange, C. de Bruin-Dickason and C. Jones, *Zeitschrift fur Anorg. und Allg. Chemie*, 2020, **646**, 603–608.
31 F. Xu, Y. X. Peng, B. Hu, T. Tao and W. Huang, *CrystEngComm*, 2012, **14**, 8023–8032.